On Hair Recognition in the Wild by Machine

Joseph Roth and **Xiaoming Liu**
Department of Computer Science and Engineering
Michigan State University, East Lansing, MI 48824
{rothjos1, liuxm}@msu.edu

Abstract

We present an algorithm for identity verification using only information from the hair. Face recognition in the wild (i.e., unconstrained settings) is highly useful in a variety of applications, but performance suffers due to many factors, e.g., obscured face, lighting variation, extreme pose angle, and expression. It is well known that humans utilize hair for identification under many of these scenarios due to either the consistent hair appearance of the same subject or obvious hair discrepancy of different subjects, but little work exists to replicate this intelligence artificially. We propose a learned hair matcher using shape, color, and texture features derived from localized patches through an AdaBoost technique with abstaining weak classifiers when features are not present in the given location. The proposed hair matcher achieves 71.53% accuracy on the LFW View 2 dataset. Hair also reduces the error of a Commercial Off-The-Shelf (COTS) face matcher through simple score-level fusion by 5.7%.

Introduction

For decades *machine-based* face recognition has been an active topic in artificial intelligence. Generations of researchers have developed a wide variety of face recognition algorithms, starting from Dr. Kanade's thesis using a shape-based approach (1973), to the appearance-based Eigenface approach (Turk and Pentland 1991), and to the recent approach that integrates powerful feature representation with machine learning techniques (Chen et al. 2013). It is generally agreed that face recognition achieves satisfying performance on the *constrained* setting, as shown by the MBGC test (Phillips et al. 2009). However, face recognition performance on the *unconstrained* scenario is still far from ideal and there have been substantial efforts to improve the state of the art, especially demonstrated by the series of developments on the benchmark Labeled Faces in the Wild (LFW) database (Huang et al. 2007).

Despite the vast amount of face recognition work, in both constrained and unconstrained scenarios, almost all algorithms rely on the internal parts of the face (e.g., eyes, nose, cheeks, and mouth), and exclude the external parts of the face, such as hair, for recognition. Only very few papers discuss the role of hair in face recognition. For example, Chen et al. (2001) show that hair can dominate the classification decision for PCA-type approaches. Yacoob and Davis (2006) quantitatively evaluate the performance of hair-based constrained face recognition. Kumar et al. (2011) present an attribute-based face verification system where hair comprises 10 out of 73 attributes for face matching. So far there is no prior work studying hair for the emerging unconstrained face recognition. This lack of study is partially attributed to the common *impression* that hair is not stable and can easily change. However, from people around us, we see ordinary people do not change hairstyle often. Hence, out of scientific curiosity, we employ a *data-driven* approach to study whether hair is indeed discriminative, i.e., we let the data tell us if the common impression is true.

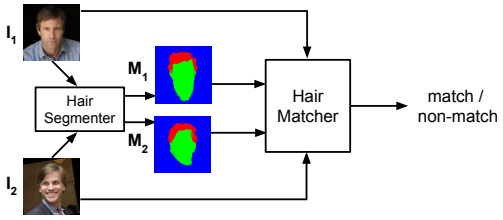

Figure 1: A *hair matcher* takes two images and their corresponding segmented hair mask and determines if they belong to the same subject or different subjects.

In contrast, there is a long history of studying the role of hair in *human-based* face recognition (Sinha and Poggio 1996; Wright and Sladden 2003; Johnston and Edmonds 2009; Toseeb, Keeble, and Bryant 2012). Intuitively, you notice when a friend cuts their hair or changes their hairstyle. Indeed, Davies, Ellis, and Shepherd (1981) show that hair is the most important single feature for recognizing familiar faces. Sinha and Poggio (1996) combine the internal part of Bill Clinton with the hair and other external features of Al Gore, and the synthesized face appears more similar to Gore. A similar study concludes that hair plays a vital role in human-based face recognition, especially for recognizing faces of your own gender (Wright and Sladden 2003).

Driven by both the scientific curiosity, as well as the discrepancy between hair-based human and machine face recognition, this paper aims to study *whether*, *how*, and *when* hair is useful for unconstrained face recognition by

a machine. On the other hand, our study is also motivated and enabled by a number of exciting recent research on hair segmentation or labeling (Scheffler, Odobez, and Marconi 2011; Lee et al. 2008; Wang, Ai, and Tang 2012; Kae et al. 2013; Wang et al. 2013), which substantially improve the segmentation accuracy on unconstrained facial images. For instance, the advanced hair labeling approach from Kae et al. (2013) achieves 95% accuracy compared to the ground truth at the superpixel level. The availability of excellent hair segmentation and the needs for improved face recognition enable us to study this interesting topic.

Unlike conventional face recognition that uses only the internal parts of two faces, this paper studies how to perform face recognition by using a complementary part, the hair regions, of two faces. We assume that a good quality hair segmentation has been conducted on two images. As shown in Fig. 1, our central task is to design a discriminative feature representation and classifier, termed "hair matcher", to compute the similarity between two hair regions. Since hair is a highly non-rigid object, we decide to use a local patch-based approach for feature representation. Given two faces aligned by their eye locations, we have a series of rays emitting from the center of two eyes and intersecting with the contour of the hair. We use the hair segmenter from Kae et al. (2013) to identify the hair mask. The intersection points will determine the local patches where we compute a rich set of carefully designed hair features, including Bag of Words (BoW)-based color features, texture features, and hair mask-based shape features. We use a boosting algorithm to select the features from local patches to form a classifier. Our boosting algorithm can abstain at the weak classifier level based on the fact that hair may not be present at some local patches (Schapire and Singer 1999).

Our work differs from the prior work of Yacoob and Davis (2006) and Kumar et al. (2011) in three aspects: 1) we focus on unconstrained face recognition with greater hair variations, 2) we employ a local patch driven approach to optimally combine a wide variety of carefully designed features rather than using global descriptors from human intelligence such as split location, length, volume, curls, etc., 3) we explicitly study the fusion of hair with face, which is critical for applying hair recognition to real-world applications.

In summary, this paper has a number of contributions:

◇ We develop a hair matcher for unconstrained face recognition and evaluate on the standard LFW database. This is the first known reported result from hair only on this de facto database of unconstrained face recognition.

◇ We demonstrate that hair and face recognition are *uncorrelated* and fail under different circumstances which allows for improvement through fusion.

◇ We use basic fusion techniques with the proposed hair matcher and a COTS face matcher and demonstrate improved face verification performance on the LFW database.

Hair Recognition Approach

Hair Matcher Framework

Given a pair of images $\mathbf{I}_i$ and $\mathbf{I}_j$, along with their corresponding hair masks $\mathbf{M}_i$ and $\mathbf{M}_j$, a hair matcher consists of a function, $F(\mathbf{I}_i(\mathbf{M}_i), \mathbf{I}_j(\mathbf{M}_j))$, that returns a large value if the images belong to the same subject, or otherwise a small value. This paper assumes that the hair mask $\mathbf{M}_i$ can be obtained automatically through a hair segmenter.

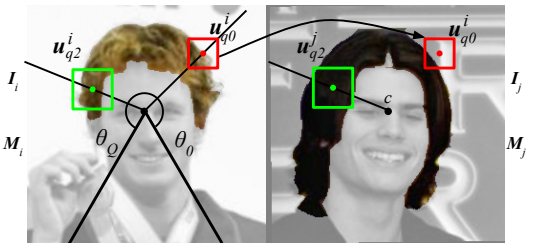

Figure 2: Patch localization: Green region $\mathbb{R}_{40}$ is extracted from the center of the ray independently for each image and is used to compute color and texture features. Red region $\mathbb{R}_{30}$ is extracted from only $\mathbf{I}_i$ and mapped to the same location in $\mathbf{I}_j$ and is used to compute shape features.

Alignment is often the first step for any object recognition system (Liu et al. 2008; Liu 2009), such that the topologically *equivalent* parts are compared with each other. Unlike rigid objects where alignment is easy w.r.t. a standard object instance, hair is a highly non-rigid object where the alignment between two hair regions does not appear straightforward. Fortunately, hair attaches to the head, which is relatively more rigid compared to hair and can be better aligned via the face. Therefore, given an image pair, we first align their face regions, and the aligned images are the input ($\mathbf{I}_i$ and $\mathbf{I}_j$) to the proposed algorithm. Specifically, in the LFW database, we choose to work on the funneled dataset (Huang, Jain, and Learned-Miller 2007) where all face regions are reasonably aligned with the in-plane rotation (roll) removed.

Patch localization: Similar to any object recognition system, the hair matcher requires an effective feature representation. We choose to use a *local* feature-based representation due to two considerations. 1) Hair may have distinct local properties (e.g., texture, shape, color) across one part of the hair region. 2) Local representation is potentially more robust to the hair segmentation error, which is typically non-uniformly distributed over the hair region.

In order to consistently localize patches for feature extraction, we propose a ray-based sampling method. As shown in Fig. 2, given the center ($\mathbf{c}$) of two average eye locations in the dataset, we define a line function $l_q(\mathbf{u}; \theta_q) = 0$ that passes through $\mathbf{c}$ with a horizontal angle θ_q. (We cannot use an image-specific eye center without violating the restricted protocol of LFW). By varying θ_q within a range, specifically $\theta_q = \frac{q}{Q}\frac{5\pi}{3} - \frac{\pi}{3}$ for $q \in [0, Q]$ and $Q = 106$, a collection of line functions are generated. This range ignores the locations beneath the face where very few images have hair. We denote the set of boundary pixels of a hair mask $\mathbf{M}$ as $\mathbf{B}$, which describes the internal and external hair lines. It is expected that in many cases the line function will intersect with $\mathbf{B}$, and the collection of intersected points of all lines is denoted as $\{\mathbf{u}_q, \mathbf{u'}_q\}$, where $l_q(\mathbf{u}_q) = l_q(\mathbf{u'}_q) = 0, \{\mathbf{u}_q, \mathbf{u'}_q\} \in \mathbf{B}$. We sample patches at five equidistant locations along each line l_q at $\mathbf{u}_{qp} = \frac{p}{4}\mathbf{u}_q + \frac{4-p}{4}\mathbf{u'}_q$ for $p \in [0, 4]$. From now on

$\{\mathbf{u}_{qp}\}$ defines the local patch centers for extracting various feature representations. Note that depending on the shape of hair, $\{\mathbf{u}_{qp}\}$ may contain empty elements for a subset of θ_q. This implies that no local feature will be extracted from these patch locations, and we will handle this missing feature issue by our classifier learning algorithm.

Feature Extraction

Hair Color Features The Fischer-Saller scale is used in physical anthropology and medicine to describe the hair color distribution, where a series of scales is defined from light blond to red blond (Hrdy 1978). Inspired by this, we use a data driven approach to learn the distribution (or codes) of hair color in our training dataset. Specifically, we convert all hair pixels within the N training images, $\{\mathbf{I}_i(\mathbf{M}_i)\}_{i\in[1,N]}$, from the RGB space to the HSV space. In order to learn the representative hair color, one would typically perform a K-means clustering in the 3-dim HSV space. However, Euclidean distances perform poorly for clustering the polar coordinates of HSV. Specifically, when the value (V) is small, colors are very similar regardless of the hue (H) or saturation (S). To remedy these issues, we scale S by V to create a conical space, and then perform K-means clustering on its Cartesian representation. As shown in Fig. 3, the resultant $d_c = 20$ color codes, $[\mathbf{s}_1, \mathbf{s}_2, \cdots, \mathbf{s}_{d_c}]$, appear to cover a wide range of typical hair colors.

Given one image $\mathbf{I}$, we use the center point along each line $\mathbf{u}_{q2}$. For each hair pixel within an $r \times r$ patch $\mathbb{R}_r$ around $\mathbf{u}_{q2}$ where $r \in \{21, 41\}$, we search for its nearest color code. For each patch, we generate a d_c-dim BoW histogram $\mathbf{f}^c_{qr} = \frac{\mathbf{h}}{||\mathbf{h}||_1}$, where
$\mathbf{h}(d) = \sum_{(u,v)\in\mathbb{R}_r} \delta(d = \arg\min_d ||\mathbf{I}(u,v) - \mathbf{s}_d||_2)\delta(\mathbf{M}(u,v) = 1)$,
and $\delta()$ is the indicator function. The collection of all patch-based color histograms constitutes the color feature for the image $\mathbf{I}$, $\mathbf{f}^c = \{\mathbf{f}^c_{qr}\}$.

Hair Texture Features Many texture features are used in vision applications and we use Gabor filter (Liu and Chaudhuri 2002), Local Binary Patterns (LBP) (Ojala, Pietikainen, and Maenpaa 2002), and an oriented gradient feature similar to Histogram of Oriented Gradients (HOG) (Dalal and Triggs 2005). Gabor filter has been widely used in face recognition as a low-level feature representation. We choose it to describe hair texture due to its capability in capturing hair orientation. Specifically, the Gabor filter is defined as:

$$\mathbf{G}_{x,y}(\lambda,\theta,\psi,\sigma,\gamma) = \exp(-\tfrac{x'^2+\gamma^2 y'^2}{2\sigma^2})\exp(i(2\pi\tfrac{x'}{\lambda}+\psi)),$$

where $x' = x\cos(\theta) + y\sin(\theta)$, $y' = -x\sin(\theta) + y\cos(\theta)$. By setting $\psi = \frac{\pi}{2}$, $\sigma = 2$, $\gamma = 0.5$, $\lambda = \{0.5, 1, \cdots, 2.5\}$, and $\theta = \{\frac{\pi}{8}, \frac{2\pi}{8}, \cdots, \pi\}$, we have 40 different Gabor filters and their convolution with an image $\mathbf{I}$ generates 40 filter responses $\mathbf{G}^I_j = \mathbf{I} * \mathbf{G}(\lambda,\theta)$. Similar to the color feature, for each patch $\mathbb{R}_r(\mathbf{u}_{q2})$, we compute the texture feature, which is a 40-dim vector $\mathbf{f}^g_{qr}$ with each element being the mean of the real part of the filter responses, i.e., $\mathbf{f}^g_{qr}(j) = \frac{1}{||\mathbf{u}||_1}\sum_{(u,v)\in\mathbb{R}_r} \mathrm{Re}(\mathbf{G}^I_j(u,v))\delta(\mathbf{M}(u,v) = 1)$.

LBP creates an 8-bit number for each $\mathbf{u}$ by thresholding the 8-neighborhood by $\mathbf{I}(\mathbf{u})$. All numbers where consecutive bits change values more than twice are mapped to the same pattern, leaving only 59 unique patterns. This mapping is denoted as $LBP_{8,2}$. A histogram of the patterns within the patch is used as the LBP feature, i.e., $\mathbf{f}^l_{qr} = \frac{\mathbf{h}}{||\mathbf{h}||_1}$, where $\mathbf{h}(j) = \sum_{(u,v)\in\mathbb{R}_r} \delta(LBP_{8,2}(u,v) = j)\delta(\mathbf{M}(u,v) = 1)$.

For HOG-like features, we compute the histogram using nine orientations evenly spaced between 0 and π. The feature $\mathbf{f}^h_{qr}$ is the normalized histogram of the sum of all gradients with the given orientation. Our system differs from Dalal's HOG in that we use the whole region $\mathbb{R}_r$ as a single cell instead of sampling multiple cells within a block. This leaves us with a $6Q$-dim texture feature $\mathbf{f}^t = \{\mathbf{f}^g_{qr}, \mathbf{f}^l_{qr}, \mathbf{f}^h_{qr}\}$ per image.

Hair Shape Features Hair shape can be described solely by the internal and external hair lines. Ideally for the genuine match, both hair lines of one image should overlap with those of the other image. However, due to the potential discrepancy in head poses, such overlap may not happen everywhere along the hair lines. To remedy this issue, one approach is to perform a 3D hair model fitting on one image, rotate the head to the same pose as the other image, and synthesize the hair lines under the new pose. Considering the challenger of 3D hair fitting for unconstrained images, we take an alternative approach to search for the local regions that have more consistent hair lines under pose variations.

Unlike the color and texture, where only the center between two hair boundary points is used for feature extraction, for the shape feature we use all five $\mathbf{u}_{qp}$ points along each line. For each point, we use the hair mask within its local patch as the shape feature, $\mathbf{f}^s_{qpr} = \mathbf{M}(\mathbf{u}), \forall\mathbf{u} \in \mathbb{R}_r(\mathbf{u}_{qp})$, where the patch size $r = \{11, 21, 31\}$.

For the color and texture, the two matching images, $\mathbf{I}_i$ and $\mathbf{I}_j$, have different patch locations for feature extraction, $\mathbf{u}^i_{q2}$ and $\mathbf{u}^j_{q2}$. In contrast, for shape, both images extract features from the *same* locations, which are $\mathbf{u}_{qp}$ of one of the two images. That is, $\mathbf{f}^i_{qpr} = \mathbf{M}_i(\mathbf{u}), \forall\mathbf{u} \in \mathbb{R}_r(\mathbf{u}^i_{qp})$ and $\mathbf{f}^j_{qpr} = \mathbf{M}_j(\mathbf{u}), \forall\mathbf{u} \in \mathbb{R}_r(\mathbf{u}^i_{qp})$ are the local shape features of $\mathbf{I}_i$ and $\mathbf{I}_j$. The shape feature for an image pair is defined as,

$$\mathbf{x}^s_{qpr}(\mathbf{u}) = \begin{cases} 1, & \text{if } \mathbf{f}^i_{qpr}(\mathbf{u}) = \mathbf{f}^j_{qpr}(\mathbf{u}) = 1, \\ 0, & \text{if } \mathbf{f}^i_{qpr}(\mathbf{u}) = \mathbf{f}^j_{qpr}(\mathbf{u}) = 0, \\ -1, & \text{otherwise,} \end{cases} \quad (1)$$

where $\mathbf{x}^s_{qpr}$ is a r^2-dim vector. This definition allows us to treat differently the pixels being both hair or both background. Note that it is important to ensure that the feature comparison is conducted only for the pixels at the same location, otherwise the hairs with different thickness would also match well based on the shape feature definition.

Given an image pair $\mathbf{I}_i$ and $\mathbf{I}_j$, we represent the visual similarity of two hair regions via the joint feature vector, $\mathbf{x} = [\mathbf{x}^c, \mathbf{x}^t, \mathbf{x}^s] = [|\mathbf{f}^c_i - \mathbf{f}^c_j|, |\mathbf{f}^t_i - \mathbf{f}^t_j|, \{\mathbf{x}^s_{qpr}\}]$. There are $2Q$ color features with the dimension of d_c, $6Q$ texture features with the dimension of 40, 59, or 9, and $15Q$ shape features with the dimension of r^2. Depending on whether two images are of the same subject, $\mathbf{x}$ will be used as a positive or negative training sample for learning a hair matcher.

Algorithm 1: Learning a hair matcher via boosting.

Data: Samples and labels $\{\mathbf{x}_n, y_n\}_{n\in[1,N]}$, with $y_n \in \{-1, +1\}$.
Result: The hair matcher classifier F.
Initialize the weights $w_n = \frac{1}{N}$, and $F = 0$.
foreach $m = 1, \cdots, M_1$ **do**
  foreach $v = 1, \cdots, 23Q$ **do**
    $\arg\min_{\mathbf{w},\tau,p} \sum_{n=1}^{N} \mathbf{1}(\mathbf{x}_n^v) w_n (f(\mathbf{x}_n^v; \mathbf{w}, \tau, p) - y_n)^2$,
    where $\mathbf{1}(\mathbf{x}_n^v) = 0$ if $\mathbf{x}_n^v$ is abstained and 1 otherwise, and

$$f(\mathbf{x}_n^v; \mathbf{w}, \tau, p) = \begin{cases} 1, & \text{if } p\mathbf{w}^\intercal \mathbf{x}_n^v > \tau, \\ -1, & \text{if } p\mathbf{w}^\intercal \mathbf{x}_n^v < \tau, \\ 0, & \text{if } f \text{ abstains on } \mathbf{x}_n^v. \end{cases} \quad (2)$$

    $W_c = \frac{1}{N}\sum_n (f(\mathbf{x}_n^v) = y_n)$,
    $W_m = \frac{1}{N}\sum_n (f(\mathbf{x}_n^v) \neq y_n)$,
    $W_a = \frac{1}{N}\sum_n (f(\mathbf{x}_n^v) = 0)$.
  Select f_m with minimal $Z = W_a + 2\sqrt{W_c W_m}$. Quit if $Z = 1$.
  If f_m uses a color feature, compute $\mathbf{A}$ via DML.
  Compute $\alpha_m = \frac{1}{2}\log(\frac{W_c}{W_m})$ and update the weights:

$$w_n = \begin{cases} \frac{w_n}{W_a\sqrt{\frac{W_m}{W_c}}+2W_m}, & \text{if } f_m \text{ misclassifies } \mathbf{x}_n, \\ \frac{w_n}{W_a\sqrt{\frac{W_c}{W_m}}+2W_c}, & \text{if } f_m \text{ classifies } \mathbf{x}_n, \\ \frac{w_n}{Z}, & \text{if } f_m \text{ abstains on } \mathbf{x}_n. \end{cases} \quad (3)$$

  Normalize the weights w_n such that $\sum_n w_n = 1$.
return $F(\mathbf{x}) = \sum_{m=1}^{M_1} \alpha_m f_m(\mathbf{x}; \mathbf{w}, \tau, p)$.

Classifier Learning

Similarity Measurement Having extracted the feature representation for both genuine matches and impostor matches, now we need to learn a classifier to separate these two classes. Given the high dimensionality of the feature space, we choose to use boosting due to its known advantage in combining both feature selection and classifier learning in one step, as well as its success in many vision problems (Viola and Jones 2004). A major part of any boosting framework is to learn weak stump classifiers. We choose to learn a simple similarity measure for a given local feature vector by projecting $\mathbf{x}_n = |\mathbf{f}_i - \mathbf{f}_j|$ to a scalar, and then performing classification by a simple threshold τ. Similar to Liu and Yu (2007), this projection can be done efficiently through Linear Discriminant Analysis (LDA) to learn a vector $\mathbf{w}$ to maximize the difference between two classes. Since higher similarity values for the genuine match is desired, a parity p is used to flip the sign after the projection:

$$s = p\mathbf{w}^\intercal \mathbf{x}_n. \quad (4)$$

Learning the LDA projection is computationally efficient, but it fails to consider the correlation between different dimensions of the local feature vector. For the texture and shape features, there is minimal correlation, but for the color features there is correlation between similar color codes especially since lighting can impact the color. Distance Metric Learning (DML) (Xing et al. 2003) is designed to learn a projection that considers the correlation among features.

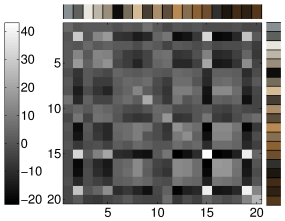

Figure 3: Example DML matrix $\mathbf{A}$. Note colors from specular reflection (e.g., Code 1 and 3) have little impact on the similarity s as all values are close to zero.

Specifically, a full rank matrix $\mathbf{A}$, rather than a vector, is learned to project the features as follows:

$$s = p(\mathbf{f}_i - \mathbf{f}_j)^\intercal \mathbf{A}(\mathbf{f}_i - \mathbf{f}_j), \quad (5)$$

according to the objective function:

$$\begin{aligned} \min_{\mathbf{A}} \quad & \sum_{(\mathbf{f_i},\mathbf{f_j})\in N^+} ||\mathbf{f}_i - \mathbf{f}_j||_{\mathbf{A}}^2 \\ \text{s.t.} \quad & \sum_{(\mathbf{f_i},\mathbf{f_j})\in N^-} ||\mathbf{f}_i - \mathbf{f}_j||_{\mathbf{A}}^2 \geq 1, \mathbf{A} \succeq 0, \end{aligned} \quad (6)$$

where N^+ and N^- are the genuine and impostor training samples respectively. Figure 3 shows one resultant $\mathbf{A}$ matrix.

Boosting with Abstaining Features One unique aspect of our problem is that for any local feature, it is possible that one image or both images of a certain pair do not have feature values, because no hair is present in that specific local patch. Therefore, we decide to use boosting with abstaining features for our problem (Schapire and Singer 1999; Smeraldi, Defoin-Platel, and Saqi 2010), which can specifically consider absent features during feature selection.

Algorithm 1 presents the key steps in our boosting-based learning. We learn a similarity measure for each individual feature in order to use the conventional stump classifier with a threshold τ and a parity p. Unlike conventional boosting, the sample with an absent feature has a classifier output of 0 (Eq. 2) and does not participate in the estimation of stump classifier parameters ($\mathbf{w}$, τ, p). The weak classifier is selected not only by the amount of samples that are classified correctly (W_c) and misclassified (W_m), but also by those that have abstained features (W_a). This prevents the feature selection from favoring a feature where many samples have abstained. Similarly, these three values also determine the updating of the sample weights. Note that for efficiency we do not compute DML for every color-based stump classifier during the iteration, but rather wait until the iteration has completed. Finally, the boosting procedure results in a hair matcher, which is a weighted summation of M_1 weak classifiers each with associated parameters ($\mathbf{w}$ or $\mathbf{A}$, τ, p).

Fusion with COTS Face Matcher

Since hair is not dependent on face occlusion or expression, we aim to create a fusion scheme where a COTS face matcher can benefit from the proposed hair matcher. We plan to fuse at the score level since that is the highest level possible with a black box COTS system.

(a) (b) (c)

Figure 5: Examples of hair matcher performance. Correct samples with the greatest $|F(\mathbf{x})|$ (a), random correct samples (b), and incorrect samples with the greatest $|F(\mathbf{x})|$ (c).

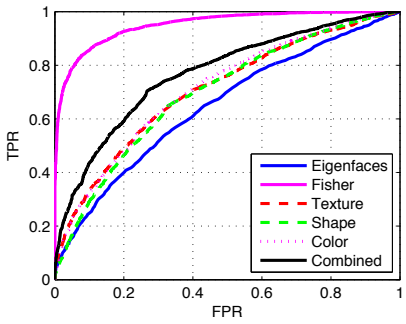

Figure 4: ROC comparison of Eigenfaces, Hair, and Fisher vector faces on LFW View 2.

The first step to fusion is to choose a suitable score-normalization. We desire a technique that reduces the effect of outliers and is also unaffected by the non-Gaussian impostor distribution of the COTS matcher. To fulfill these needs, we choose to use the tanh normalization (Jain, Nandakumar, and Ross 2005), which is based on the mean μ and standard deviation σ of the genuine training samples using:

$$F'(\mathbf{x}) = \frac{1}{2}\left[\tanh\left(0.01\left(\frac{F(\mathbf{x})-\mu}{\sigma}\right)\right)+1\right]. \quad (7)$$

The second step is to combine the normalized scores, where standard techniques include min, max, and mean. Since we have enough training data, we use a Support Vector Machine (SVM) with a standard radial basis kernel to form a final classification decision instead.

There are certain instances where either hair or face can produce poor results, e.g., obscurity through a hat or sunglasses. In the future, we can further improve the fusion performance by estimating *quality metrics* for both face and hair and feed them to the SVM. This will make a decision based not only on the raw score, but also on which metric will work best for the given conditions.

Experimental Results

In this section, we evaluate the proposed hair matcher in the unconstrained face recognition scenario. We seek to understand when the hair matcher succeeds and under what scenarios it can improve face recognition.

Hair Matcher

To evaluate the proposed algorithm, we use the de facto database for unconstrained face recognition, LFW (Huang et al. 2007). LFW is popular due to its unconstrained nature, difficulty, well-defined protocol, and the availability of results of prior work. To ensure hair alignment between two images, the funneled version of LFW is used (Huang, Jain, and Learned-Miller 2007). We use the hair segmenter from Kae et al. (2013). The database consists of $13,233$, 250x250 pixel images from $5,749$ individuals. We follow the restricted View 2 protocol, where $3,000$ genuine matches and $3,000$ impostor matches are divided into 10 equal size partitions for cross validation.

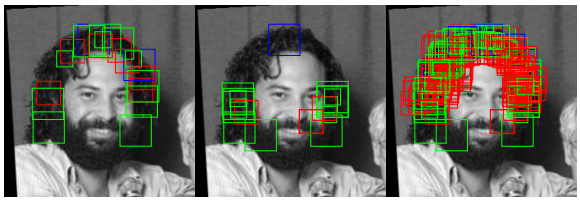

(a) (b) (c)

Figure 6: Distribution of shape (red), texture (green), and color (blue) features chosen by boosting. First 20 (a), top 20 by weights α (b), and all 200 (c) features.

We employ the standard Receiver Operating Characteristic (ROC) curve for performance evaluation. The ROC curve is defined on two axes: False Positive Rate (FPR), the fraction of impostor matches incorrectly accepted to be genuine, and True Positive Rate (TPR), the fraction of genuine matches correctly classified as genuine. To summarize the ROC curve, we use the Equal Error Rate (EER), which is when FPR equals $1-$TPR, and the accuracy ($1-$EER).

Figure 4 displays the performance of the proposed hair matcher with the original Eigenfaces (Turk and Pentland 1991) and the state-of-the-art Fisher vector faces (Simonyan et al. 2013). We run the hair matcher using shape, color, and texture features independently in order to demonstrate their individual effectiveness. They perform nearly the same, and when combined, the learned hair matcher achieves 71.53% accuracy. As no other hair technique is designed for the unconstrained setting nor tested on LFW, this is the first reported result using a hair matcher on LFW. Figure 5 displays samples where the hair matcher succeeds and fails.

Selected Features: Figure 6 shows the features selected by boosting. This specific matcher selects 123 shape features, 69 texture features, and 8 color features. Even though color performs well by itself, it has fewer overall selections. We hypothesize that this is due to DML only being computed if

Figure 9: Sweetspot pairs: Samples where fusion successfully corrects misclassified pairs by the COTS system.

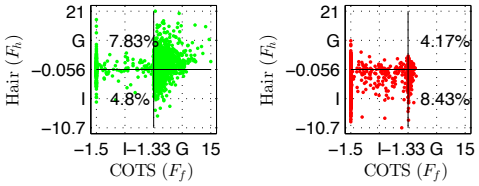

(a) (b)

Figure 7: Distributions of COTS and hair scores for genuine (a) and impostor samples (b). G and I on the axes refer to matcher's classification decision as genuine or imposter.

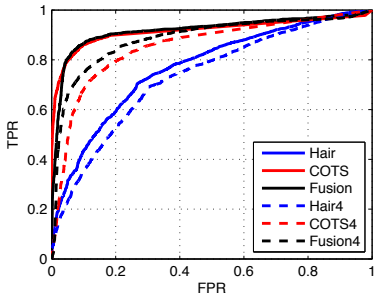

Figure 8: ROC comparison of COTS, hair matcher, and fused results on full and quarter resolution images.

a color feature is chosen through the weaker LDA. Despite this disadvantage, color is still important, since a color feature near the top of the head is almost always chosen first with a high weight. Because the boosting algorithm may abstain, it is possible to have higher weighted features appearing at later iterations. As seen in the middle image, these top weighted features tend to be beneath the ears where fewer images have hair, but when present is highly discriminative.

Fusion with COTS Face Matcher

The proposed hair matcher performs well, but it is still behind the state-of-the-art performance of face recognition. We seek to determine the usefulness of the hair matcher by fusing with PittPatt V5.2 (pit 2011), one of the best performing COTS face matchers. Figure 7 shows the joint distribution of F_f and F_h.The Pearson correlation coefficient is 0.4, which indicates low correlation, and thus fusion has the potential to improve performance. Each axis is scaled piecewise linearly to provide equal space for the genuine and impostor decisions and the overlay shows the percentage of samples occurring in the cases where COTS fails. We call the regions where hair succeeds but face fails the *sweetspot* and 8.13% of testing image pairs fall into these regions. If there exists a perfect fusion scheme, hair would improve the performance of the COTS to 95.5%, which indicates the great promise of fusing hair with face recognition.

Using SVM on $\tanh$ normalized scores, we generate the ROC curve in Fig. 8. This fusion scheme increases the COTS performance from 87.38% to 88.10%, which is a 5.7% reduction of the error. Although minor in improvement, the paired t-test has a *statistically significant* p-value of 0.014. This demonstrates that hair is able to *improve* the face recognition performance. In the future, we will develop face and hair quality metrics to better predict sweetspot pairs.

Table 1: Accuracy comparison

Matcher	Hair	COTS	Fused
Full resolution	71.53%	87.38%	88.10%
Quarter resolution	68.63%	79.69%	82.37%

Figure 9 demonstrates examples where the fused matcher corrects errors made by the COTS. We make the following remarks from these examples. Face recognition can be significantly hindered by obstructions (e.g., sunglasses), poor focus, expression, lighting, and pose variation. Hair works without respect to expression or obstructions, and the degradation due to pose, focus, and lighting is less than face.

Low Resolution: To examine the degradation of the proposed hair matcher w.r.t. image resolution, we downsample the LFW database to 63×63 pixel images (quarter resolution). Since we are interested only in the performance of the hair matcher and not hair segmentation, we also downsample the hair masks directly. The reported results will be achievable if/when hair segmentation works at the low resolution. At this resolution, the COTS matcher fails to enroll (FTE) and produces no score for 14.8% of the pairs. To report the performance of COTS, we flip a coin when this occurs and assign the pair a random score from either the genuine or impostor distribution. When COTS produces a score, the accuracy is 84.86%, but the FTE cases cause the accuracy to drop to 79.69%. Hair recognition degrades gracefully at the reduced resolution, so we modify the fusion scheme to use only F_h whenever FTE occurs. Fusion appears to be more effective and has an error reduction of 13.20%. The exact performance results are presented in Tab. 1 and Fig. 8.

Conclusions

With a structured and data-driven approach, we presented the first work for automated face recognition using only hair features in the unconstrained setting. On the de facto LFW dataset, we showed the usefulness of our fully automatic hair matcher by itself and by improving a COTS face matcher. Through the answers of *whether*, *how* and *when* hair is useful for unconstrained face recognition, this work made a notable contribution to this important problem, and warranted further study on hair, the often-ignored visual cue.

Acknowledgement

We thank Andrew Kae and Erik Learned-Miller in kindly providing the hair segmentation masks of the LFW images.

References

Chen, L.-F.; Liao, H.-Y. M.; Lin, J.-C.; and Han, C.-C. 2001. Why recognition in a statistics-based face recognition system should be based on the pure face portion: a probabilistic decision-based proof. *Pattern Recognition* 34(7):1393 – 1403.

Chen, D.; Cao, X.; Wen, F.; and Sun, J. 2013. Blessing of dimensionality: High-dimensional feature and its efficient. compression for face verification. In *Proc. IEEE Conf. Computer Vision and Pattern Recognition (CVPR)*, 3025–3032.

Dalal, N., and Triggs, W. 2005. Histograms of oriented gradients for human detection. In *Proc. IEEE Conf. Computer Vision and Pattern Recognition (CVPR)*, volume 1, 886–893.

Davies, G.; Ellis, H.; and Shepherd, J. 1981. *Perceiving and Remembering Faces*. New York: Academic Press.

Hrdy, D. 1978. Analysis of hair samples of mummies from semna south. *American J. of Physical Anthropology* 49:277–282.

Huang, G. B.; Ramesh, M.; Berg, T.; and Learned-Miller, E. 2007. Labeled faces in the wild: A database for studying face recognition in unconstrained environments. Technical Report 07-49, University of Massachusetts, Amherst.

Huang, G. B.; Jain, V.; and Learned-Miller, E. 2007. Unsupervised joint alignment of complex images. In *Proc. Int. Conf. Computer Vision (ICCV)*, 1–8.

Jain, A. K.; Nandakumar, K.; and Ross, A. 2005. Score normalization in multimodal biometric systems. *Pattern Recognition* 38(12):2270–2285.

Johnston, R. A., and Edmonds, A. J. 2009. Familiar and unfamiliar face recognition: A review. *Memory* 17(5):577–596.

Kae, A.; Sohn, K.; Lee, H.; and Learned-Miller, E. 2013. Augmenting CRFs with Boltzmann machine shape priors for image labeling. In *Proc. IEEE Conf. Computer Vision and Pattern Recognition (CVPR)*, 2019–2026.

Kanade, T. 1973. *Picture Processing System by Computer Complex and Recognition of Human Faces*. Ph.D. Dissertation, Kyoto University, Kyoto, Japan.

Kumar, N.; Berg, A.; Belhumeur, P. N.; and Nayar, S. 2011. Describable visual attributes for face verification and image search. *IEEE Trans. Pattern Anal. Mach. Intell.* 33(10):1962–1977.

Lee, K.-C.; Anguelov, D.; Sumengen, B.; and Gokturk, S. 2008. Markov random field models for hair and face segmentation. In *Proc. Int. Conf. Automatic Face and Gesture Recognition (FG)*, 1–6.

Liu, C., and Chaudhuri, A. 2002. Reassessing the 3/4 view effect in face recognition. *Cognition* 83(1):31–48.

Liu, X., and Yu, T. 2007. Gradient feature selection for online boosting. In *Proc. Int. Conf. Computer Vision (ICCV)*, 1–8.

Liu, X.; Yu, T.; Sebastian, T.; and Tu, P. 2008. Boosted deformable model for human body alignment. In *Proc. IEEE Conf. Computer Vision and Pattern Recognition (CVPR)*, 1–8.

Liu, X. 2009. Discriminative face alignment. *IEEE Trans. Pattern Anal. Mach. Intell.* 31(11):1941–1954.

Ojala, T.; Pietikainen, M.; and Maenpaa, T. 2002. Multiresolution gray-scale and rotation invariant texture classification with local binary patterns. *IEEE Trans. Pattern Anal. Mach. Intell.* 24(7):971–987.

Phillips, P. J.; Flynn, P. J.; Beveridge, J. R.; Scruggs, W. T.; O'Toole, A. J.; Bolme, D.; Bowyer, K. W.; Draper, B. A.; Givens, G. H.; Lui, Y. M.; Sahibzada, H.; Scallan, Iii, J. A.; and Weimer, S. 2009. Overview of the multiple biometrics grand challenge. In *Proc. Int. Conf. Biometrics (ICB)*, 705–714.

2011. PittPatt Software Developer Kit, http://www.pittpatt.com.

Schapire, R., and Singer, Y. 1999. Improved boosting algorithms using confidence-rated predictions. *Mach. Learning* 37(3):297–336.

Scheffler, C.; Odobez, J.-M.; and Marconi, R. 2011. Joint adaptive colour modelling and skin, hair and clothing segmentation using coherent probabilistic index maps. In *Proc. British Machine Vision Conf. (BMVC)*, 53.1–53.11.

Simonyan, K.; Parkhi, O. M.; Vedaldi, A.; and Zisserman, A. 2013. Fisher vector faces in the wild. In *Proc. British Machine Vision Conf. (BMVC)*, 8.1–8.12.

Sinha, P., and Poggio, T. 1996. I think i know that face... *Nature* 384:404.

Smeraldi, F.; Defoin-Platel, M.; and Saqi, M. 2010. Handling missing features with boosting algorithms for protein-protein interaction prediction. In *Data Integration in the Life Sciences*, 132–147. Springer.

Toseeb, U.; Keeble, D. R.; and Bryant, E. J. 2012. The significance of hair for face recognition. *PLoS ONE* 7(3):e34144.

Turk, M., and Pentland, A. 1991. Eigenfaces for recognition. *Journal of Cognitive Neuroscience* 3(1):71–86.

Viola, P., and Jones, M. 2004. Robust real-time face detection. *Int. J. Comput. Vision* 57(2):137–154.

Wang, N.; Ai, H.; and Tang, F. 2012. What are good parts for hair shape modeling? In *Proc. IEEE Conf. Computer Vision and Pattern Recognition (CVPR)*, 662–669.

Wang, D.; Shan, S.; Zhang, H.; Zeng, W.; and Chen, X. 2013. Isomorphic manifold inference for hair segmentation. In *Proc. Int. Conf. Automatic Face and Gesture Recognition (FG)*, 1–6.

Wright, D. B., and Sladden, B. 2003. An own gender bias and the importance of hair in face recognition. *Acta Psychologica* 114(1):101 – 114.

Xing, E. P.; Ng, A. Y.; Jordan, M. I.; and Russell, S. 2003. Distance metric learning, with application to clustering with side-information. In *Advances in Neural Information Processing Systems (NIPS)*, 505–512.

Yacoob, Y., and Davis, L. 2006. Detection and analysis of hair. *IEEE Trans. Pattern Anal. Mach. Intell.* 28(7):1164–1169.